The chromosome 16p12.2–p11.2 deletion syndrome 7.1- to 8.7 Mb [MIM#613604] is distinct from 16p11.2 deletion syndrome. Hernando et al. [2002] reported the first case of multiple congenital anomalies associated with a deletion of 16p11.2 confirmed by array comparative genomic hybridization (CGH). Ballif et al. [2007], Battaglia et al. [2009], and Hempel et al. [2009] reported on further patients with a 16p12.2–p11.2 deletion. Minor facial anomalies, feeding difficulties, a significant delay in speech development, and recurrent ear infections are common symptoms of the 16p12.2–p11.2 deletion syndrome.

Reciprocal duplications of 16p12.2–p11.2 have been reported in some patients with mild to severe intellectual disability, ASD, and dysmorphic features [Engelen et al., 2002; Finelli et al., 2004; Ballif et al., 2007; Tabet et al., 2012; Barber et al., 2013]. The 16p12.2–p11.2 duplication syndrome shows variable phenotype.

We have identified a patient with a 16p12.2–p11.2 deletion and a patient with 16p12.2–p11.2 duplication using a high density oligonucleotide SNP array. The patient with deletion shared clinical features with previously reported patients. The patient with the duplication showed ASD and dysmorphic features. The duplicated region did not include the 16p11.2 region carrying susceptibility to autism. We reviewed and discussed the clinical manifestations of the two 16p12.2–p11.2 chromosomal aberrations.

CLINICAL REPORT

Patient 1 (16p12.2–p11.2 Deletion)

The 3-year-old male proband was the first-born child of a 26-year-old mother and a 30-year-old father, both healthy and non-consanguineous. After an uncomplicated pregnancy, he was born at 37 weeks of gestation by induced delivery. His length was 53 cm (90th centile). His birth weight was 1,770 g (25th centile). After birth, cardiac murmur was noticed. Echocardiography revealed VSD. Cardiac surgery was carried out successfully at 6 months of age. His developmental milestone was delayed. He showed muscle hypotonia. Head control was achieved at 10 months of age. He sat unsupported at 2 years of age. Independent walking was not possible. He spoke no meaningful words. His global development quotient was 20 at 2 years of age. Autistic features were not seen. He showed common clinical features of the 16p12.2–p11.2 deletion syndrome (Table I). Physical examination identified dysmorphic

TABLE I. Clinical Findings in Patients with 16p12.2–p11.2 Deletion Syndrome

		Ballif et al. [2007]						
	Hernando et al. [2002]	Subject 1	Subject 2	Subject 3	Subject 4	Battaglia et al. [2009]	Hempel et al. [2009]	Present patient 1
Size of deletion [Mb]		8.7	7.1	7.8	7.8	8.2	7.7	7.7
Age of diagnosis	5 months (died)	13 years 8 months	13 years 9 months	3 years 1 month	2 years 19 months	6 years	13 years 3months	3years
Gender	M	F	F	F	F	F	M	M
Delay in motor development		+	+	+	+	+	+	+
Hypotonia		+	−	+	+	+	+	+
Intellectual disability		+	+	+	+	+	+	+
Severe speech delay		+	+	+	+	+	+	+
Autism spectrum disorders		−	−	−	−	−	−	−
Growth								
Height (centile)		3rd	<3rd	25–50th	25th	50th	50th	10–25th
Weight (centile)		3rd	10–25th	50th	3rd	25th	50th	3rd
Head circumference (centile)		10th	25th	25th	8th	30th	50th	10th
Facial appearance								
Flat face	+	+	+	+	−	+	+	+
High fore head/frontal bossing	+	+	−	+	+	−	+	+
Downslanting palpebral fissures		+	+	+	+	−	−	+
Epicantal folds		+	−	+	+	−	−	−
Deep set eyes		+	−	−	+	+	+	−
Low-set, malformated ears	+	+	−	+	+	+	+	+
Small mouth							+	−
Micrognathia	+						−	
Congenital cardiac anomalies	+	+	−	−	+	−	−	+
Gastrointestinal problems								
Feeding difficulties		+	+	+	+	+	+	+
Gastro esophageal reflux		+	+	+	+	−	−	−
Hands								
Single palmar creases		+	+	+	−	+	−	−
Camptodactyly		+	+	−	−	−	−	−
Other problems								
Recurrent ear infections		+	+	+	+	+	+	+
Hearing impairment		+	−	−	−	−	+	−

features, including a flat face, downslanting palpebral fissures, low-set posteriorly rotated ears, and a thin upper lip vermilion (Fig. 1). Hearing and visual acuity were normal. His weight was 9.3 kg (−1.9 SD), and his length was 82.6 cm (−0.9 SD). His head circumference was 46.5 cm (−1.1 SD). Routine laboratory tests were normal. Neuroradiological analysis revealed no significant abnormalities. Conventional cytogenetic examination of G-banded chromosomes from peripheral blood lymphocytes was normal. Microarray analyses were performed to reveal submicroscopic chromosomal aberrations.

Patient 2 (16p12.2–p11.2 Duplication)

The patient, a 9-year-old girl, was born to non-consanguineous healthy Japanese parents. Her family history was unremarkable. She was born at 38 weeks' gestation. Her birth weight was 3,200 g. Her gross development was delayed. She started to walk independently at 18 months old. Her development in speech and social interaction were retarded. At 4 years of age, she was diagnosed with ASD. G-banded karyotyping revealed a normal female karyotype. Brain MRI was normal. EEG showed epileptic discharges, but she was free from epileptic seizures. She visited our hospital for further medical studies. Her dysmorphic features included a round face, a flat nasal bridge, full cheeks, a wide philtrum, a wide mouth, a pointed chin, fetal pads on fingers and toes, and generalized hypertrichosis (Fig. 2). Her height, weight, and head circumference were 119 cm (−2.3 SD), 22.8 kg (−1.2 SD), and 54.2 cm (+1.5 SD), respectively. Relative macrocephaly was noted. She had difficulties with daily activities. In addition, impaired social interaction, poor social skills, and strict adherence to routine behaviors were noted. She was again diagnosed with ASD according to the DSM–VI criteria. Her DQ was 76 according to the standard Japanese method. Recently, her communication skill improved. Microarray analyses were performed to reveal submicroscopic chromosomal aberrations.

MATERIALS AND METHODS

With written informed consent, genomic DNA was obtained from blood leukocytes. A copy number analysis was performed using the

FIG. 1. a,b,c: Facial appearance of Patient 1 with the 16p12.2–p11.2 deletion at 2 years of age. He shows dysmorphic features, including a flat face, downslanting palpebral fissures, low-set posteriorly rotated ears, and a thin upper lip vermilion. (Permission for presentation has been obtained from his parents).

FIG. 2. a,b: Facial appearance of Patient 2 with the 16p12.2–p11.2 duplication. Her features included a round face, a flat nasal bridge, full cheeks, wide philtrum, a wide mouth, and a pointed chin. c: Fetal pads of the fingers were observed. (Permission for presentation has been obtained from her parents).

CytoScan HD Array (Affymetrix, Santa Clara, CA) which features 2.7 million genetic markers covering the whole human genome. Genomic DNA of the patients was diluted to 50 μg/μl and processed according to the protocol (Affymetrix Cytogenetics Copy Number Assay User Guide) supplied by Affymetrix. The data were analyzed with the Chromosome Analysis Suite software (Affymetrix).

RESULTS

The SNP array analysis confirmed aberrations on the short arm of chromosome 16. The karyotype of Patient 1 was 46, XY, arr 16p12.2p11.2(21,306,156–29,053,253) × 1 (hg19) (Fig. 3). The deletion size was 7.7 Mb. The segment contained OMIM disease genes (*OTOA*, *SCNN1G*, *SCNN1B*, *COG7*, *EARS2*, *PALB2*, *IL4R*, *IL21R*, *CLN3*, *TUFM*, *SH2B1*, *ATP2A1*, and *CD19*). The karyotype of Patient 2 was 46, XX, arr 16p12.2p11.2 (21,516,366–28,234,120) × 3 (hg19) (Fig. 4). The duplication size was 6.7 Mb. The segment contained OMIM disease genes (*OTOA*, *SCNN1G*, *SCNN1B*, *COG7*, *EARS2*, *PALB2*, *IL4R*, and *IL21R*). The duplicated region of Patient 2 was smaller than the deleted region of Patient 1. *SH2B1*, *ATP2A1*, and *CD19* were not included in the duplication. These copy number variations were confirmed by FISH analysis (Fig. 5). In both families, the parents did not have the abnormalities.

DISCUSSION

The chromosome 16p12.2–p11.2 deletion syndrome 7.1 to 8.7 Mb [MIM#613604] (21.4 to 29.3 Mb) is a new syndrome resulting from non-allelic homologous recombination. The deleted segment is distal to the 16p11.2 deletion syndrome region and is distinguished from the 16p11.2 deletion syndrome which is associated with autism [Kumar et al., 2008; Marshall et al., 2008].

Hernando et al. [2002] reported the first case of multiple congenital anomalies associated with a deletion of 16p11.2 confirmed by array CGH. The male infant showed severe intrauterine growth retardation and dysmorphic features. The patient died at the age of 5 months due to cardiac disease. Ballif et al. [2007] identified a recurrent de novo pericentromeric deletion of

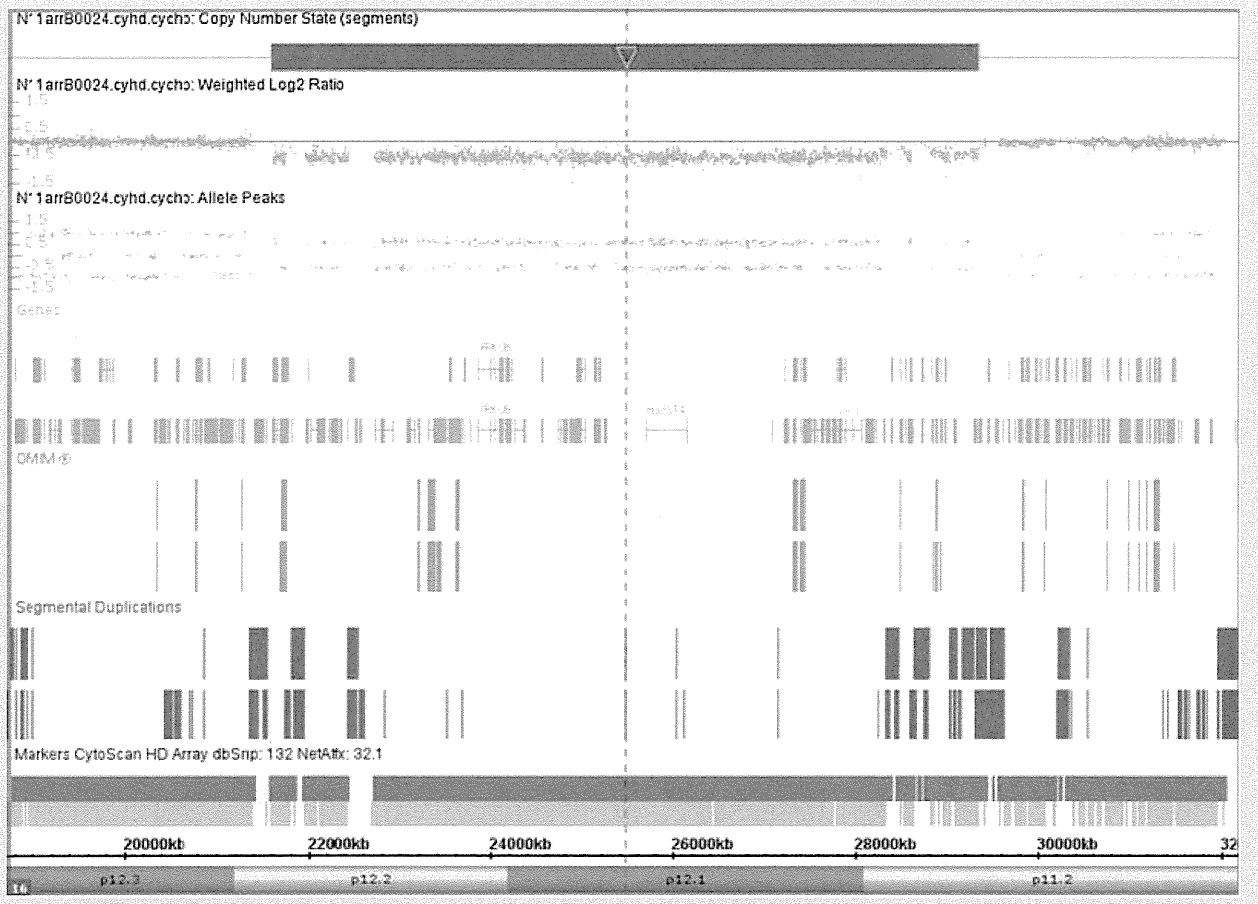

FIG. 3. Results of the SNP array analysis of Patient 1. The red bar indicates the 16p12.2–p11.2 deletion. The deletion size was 7.7 Mb. The segment contained OMIM disease genes (*OTOA, SCNN1G, SCNN1B, COG7, EARS2, PALB2, IL4R, IL21R, CLN3, TUFM, SH2B1, ATP2A1*, and *CD19*).

16p12.2–p11.2 in four individuals with developmental disabilities by array-CGH. The four patients had common clinical features. Battaglia et al. [2009] and Hempel et al. [2009] reported on further patients with a 16p12.2–p11.2 deletion.

Dysmorphic features including flat face, feeding difficulties, significant delay in speech development, and recurrent ear infections are common symptoms of the 16p12.2–p11.2 deletion syndrome. Some patients have anxiety, irritability, hyperactivity, short attention ability, and introverted behavior. However, ASD is not described in the patients. Patient 1 shared many of the clinical findings in these reports (Table I). Our result further confirmed that the 16p12.2–p11.2 deletion is responsible for a distinct multiple congenital anomalies and intellectual disability (MCA/ID) syndrome without autistic features.

The distal breakpoint of these patients was 21.4 Mb from the 16p telomere. The proximal breakpoints of these patients were 28.3–29.3 Mb from the 16p telomere and differed in the 16p11.2 region. The distal and the proximal breakpoint of Patient 1 was 21.3 Mb and 29.1 Mb from the 16p telomere, respectively.

Some disease-causing genes are included in the deleted region. Hempel et al. [2009] speculated that heterozygosity of the *OTOA* gene may cause hearing impairment in some patients. Herterozygous deletion of *CD19* may lead to recurrent ear infections. Patient 1 had recurrent ear infections. Routine laboratory investigations revealed no immunological abnormalities. Deletions encompassing the *SH2B1* gene were recently reported in early-onset obesity [Bochukova et al., 2010]. Although the *SH2B1* gene was deleted in Patient 1, he was not obese due to feeding difficulties. We should be careful for the later onset obesity.

Reciprocal duplications of 16p12.2–p11.2 have been reported in some patients with ASD and dysmorphic features [Engelen et al., 2002; Finelli et al., 2004]. However, the precise boundaries of the duplication were not defined because they were studied only by standard cytogenetic techniques. Tabet et al. [2012] reported two monozygotic twins carrying a de novo 16p12.2–p11.2 duplication of 8.95 Mb (21.28–30.23 Mb) encompassing both the 16p11.2 and 16p12.2–p11.2 regions. The twins exhibited ASD, severe intellectual disabilities, and dysmorphic features,

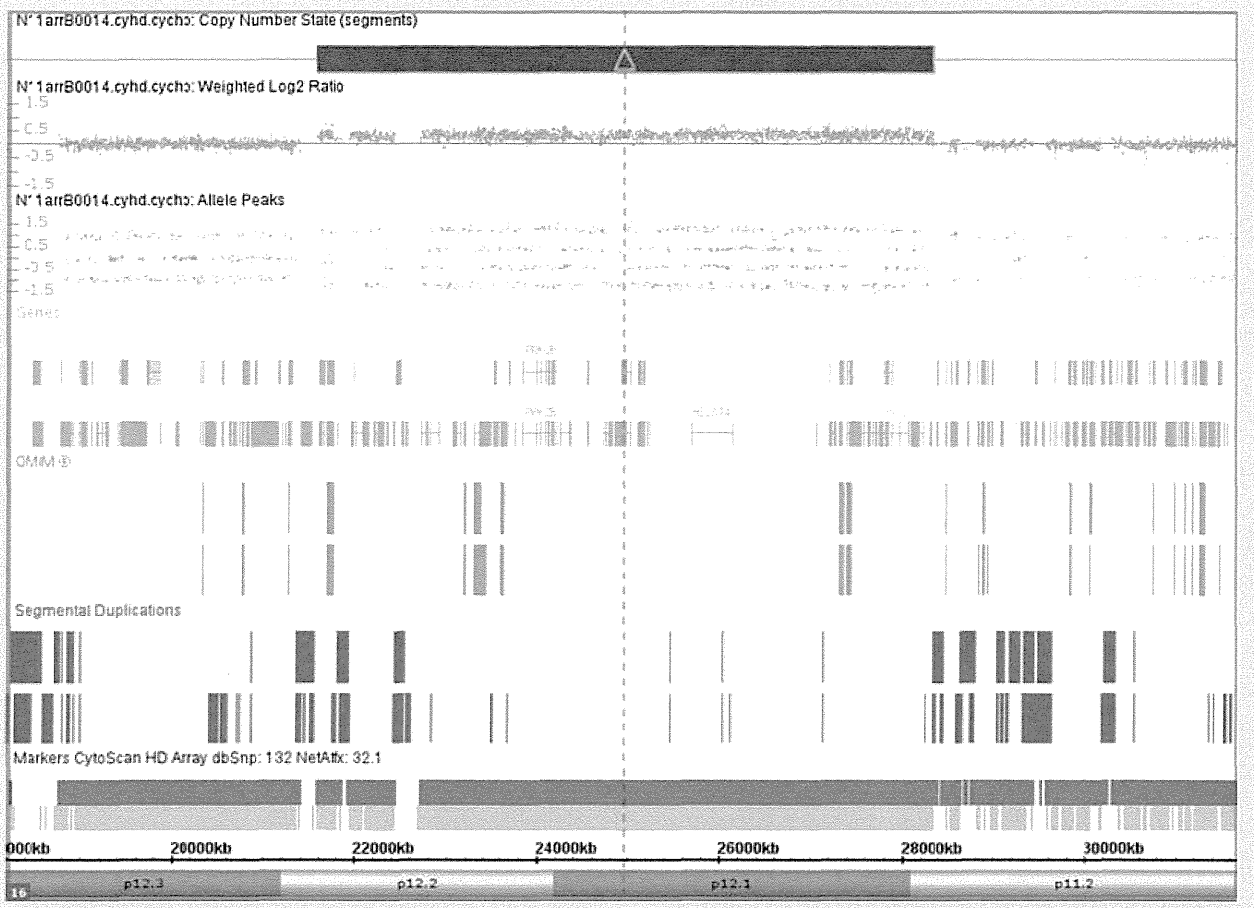

FIG. 4. Results of the SNP array analysis of Patient 2. The blue bar indicates the 16p12.2–p11.2 duplication. The duplication was 6.7 Mb. The segment contained OMIM disease genes (*OTOA*, *SCNN1G*, *SCNN1B*, *COG7*, *EARS2*, *PALB2*, *IL4R*, and *IL21R*). The duplicated region of Patient 2 was included in the deleted region of Patient 1. *SH2B1*, *ATP2A1*, and *CD19* were not included in the duplication.

including a triangular face, deep-set eyes, a large and prominent nasal bridge, and a tall, slender build. Barber et al. [2013] reported further two patients with duplication. One patient was a girl of 18 with autism, moderate ID, behavioral difficulties, dysmorphic features, and 7.71 Mb duplication. Another patient had 7.81 Mb duplication, speech delay, and obsessional behavior as a boy and, as an adult, short stature, macrocephaly and mild dysmorphism. Barber et al. [2013] suggested that the 16p12.2–p11.2 duplication syndrome is a recurrent genomic disorder with a variable phenotype.

Molecularly defined patients with the 16p12.2–p11.2 duplication syndrome are summarized in Table II. Facial features of the 16p12.2–p11.2 duplication syndrome are different among patients. Common dysmorphisms reported by Barber et al. [2013] included a depressed, broad or large nasal bridge, upslanting or narrow palpebral features, hypertelorism, and a long or tented philtrum. Patient 2 had dysmorphic features characterized by a round face, a flat nasal bridge, full cheeks, a wide philtrum, a wide mouth, a pointed chin, generalized hypertrichosis, and fetal finger pads. She

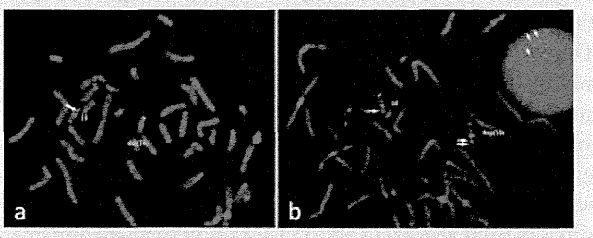

FIG. 5. A FISH analysis was performed to confirm the copy number changes. a: The red signal covering RP11-281K19 (*RBBP6*) [chr16:24,439,760–24,647,914] was deleted in patient 1. b: The red signal covering RP11-281K19 (*RBBP6*) was duplicated in Patient 2. The green signal indicates the 16q24.3 subtelomeric probe, GS-240G10. Arrows indicate RP11-281K19 (*RBBP6*).

TABLE II. Clinical Findings in Patients with 16p12.2–p11.2 Duplication Syndrome

	Finelli et al. [2004] Patient 1	Ballif et al. [2007] Subject 5	Tabet et al. [2012] Patient 2 (MZ twin)	Tabet et al. [2012] Patient 3 (MZ twin)	Barber et al. [2013] Patient 1	Barber et al. [2013] Patient 2	Present patient 1
Size of duplication [Mb]	8	5.7 Mb triplication, 1.1 Mb duplication	8.95	8.95	7.71–8.07	7.81–8.37	6.7
Age of diagnosis	25 years	10 years	17 years	18 years	15 years	45 years	9 years
General							
Gender	M	F	M	M	F	M	F
Development/neurological							
Developmental delay	+	+	+	+	+	+	+
Intellectual diability	Severe	Severe	Severe	Severe	Moderate	+	Mild
Epilepsy	+				−	−	−
EEG abnormalities	+				−		+
Autism spectrum disorders	+	+	+	+	+	−	+
Obsessive behavior	+				+	+	+
Stereotype behavior	+	+	+	+	+		
Social problems	+	+	+	+	+		−
Growth							
Height	<3rd centile	−3 to −4 SD	normal	normal	<*P*25	0.4th centile	−2.3 SD
Weight	<3rd centile	−2 SD	−2 SD	−1 SD	<*P*25		−1.2 SD
Head circumference	25th centile	−1 SD	−1 SD	−1 SD	<*P*50	Macro	1.5 SD
Facial appearance							
Round face		+	−	−			+
Triangular glabella		−	+	+			−
Promient glabella		−	+	+	+		−
Depresssed/large/broad nasal bridge	+	+	+	+	+		+
Upslanting palpebral fissures		−	+	+			−
Deep set eye		−	+	+			−
Hypertelorism	+	+	+	+			−
Nystagmus/Strabisums		+	+	+	+	+	−
Anteverted nares		+			+		−
Upper lip anomaly	+	+			−		−
Low set ears	−				−		+
Wide/large mouth	+	+					+
Full cheeks		+					+
Micro/retrognathia		−	−	−	−	+	−
Finger/hand anomalies	+	Fetal pads	+	+	−	Brachydactyly	Fetal pads
Generalized hypertrichosis							+

shared some features with other reported patients. Fetal finger pads have been found in one of the patients reported by Ballif et al. [2007]. Our results further support the evidence that ID, ASD, dysmorphic features, short stature, and anomalies of the hands and fingers are common in the 16p12.2–p11.2 duplication syndrome. However, intellectual disabilities in Patient 2 were very mild. Her communicating skill improved after 8 years old. Duplication in our patient did not include the 16p11.2 region carrying susceptibility to ASD and *SH2B1*. We suppose that differences in the proximal breakpoint may contribute to the severity of intellectual disabilities. Increased dosage of one or more genes in the duplicated region might contribute to ASD.

Delay in motor development is a constant feature of the 16p12.2–p11.2 deletion syndrome. Early development of the twins reported by Tabet et al. [2012] was normal, with walking at 15 months. The patient reported by Barber et al. [2013] walked at 13 months. Patient 2 started to walk independently at 18 months old. Delay in motor development is not considered to be a serious problem in the 16p12.2–p11.2 duplication syndrome.

Barber et al. [2013] suggested that the duplications *Polo-like kinase 1* (*PLK1*) might have an effect on neuronal development and microcephaly in human. However, one of the patients reported by them had macrocephaly and our patient also had relative macrocephaly.

We posit that the 16p12.2–p11.2 duplication is a new clinical entity with ASD due to non-allelic homologous recombination. The deletion is a MCA/ID syndrome. More patient studies will be needed to further define the syndrome.

ACKNOWLEDGMENTS

We thank for the family for their cooperation. This study was supported by the Health and Labor Research Grants in 2012 by Ministry of Health, Labor, and Welfare in Japan.

REFERENCES

Bachmann-Gagescu R, Mefford HC, Cowan C, Glew GM, Hing AV, Wallace S, Bader PI, Hamati A, Reitnauer PJ, Smith R, Stockton DW, Muhle H, Helbig I, Eichler EE, Ballif BC, Rosenfeld J, Tsuchiya KD. 2010. Recurrent 200-kb deletions of 16p11.2 that include the SH2B1 gene are associated with developmental delay and obesity. Genet Med 12:641–647.

Ballif BC, Hornor SA, Jenkins E, Madan-Khetarpal S, Surti U, Jackson KE, Asamoah A, Brock PL, Gowans GC, Conway RL, Graham JM, Jr. Medne L, Zackai EH, Shaikh TH, Geoghegan J, Selzer RR, Eis PS, Bejjani BA, Shaffer LG. 2007. Discovery of a previously unrecognized microdeletion syndrome of 16p11.2-p12.2. Nat Genet 39:1071–1073.

Barber JC, Hall V, Maloney VK, Huang S, Roberts AM, Brady AF, Foulds N, Bewes B, Volleth M, Liehr T, Mehnert K, Bateman M, White H. 2013. 16p11.2-p12.2 duplication syndrome; a genomic condition differentiated from euchromatic variation of 16p11.2. Eur J Hum Genet 21:182–189.

Battaglia A, Novelli A, Bernardini L, Igliozzi R, Parrini B. 2009. Further characterization of the new microdeletion syndrome of 16p11.2-p12.2. Am J Med Genet A 149A:1200–1204.

Bochukova EG, Huang N, Keogh J, Henning E, Purmann C, Blaszczyk K, Saeed S, Hamilton-Shield J, Clayton-Smith J, O'Rahilly S, Hurles ME, Farooqi IS. 2010. Large, rare chromosomal deletions associated with severe early-onset obesity. Nature 463:666–670.

Engelen JJ, de Die-Smulders CE, Dirckx R, Verhoeven WM, Tuinier S, Curfs LM, Hamers AJ. 2002. Duplication of chromosome region (16) (p11.2--> p12.1) in a mother and daughter with mild mental retardation. Am J Med Genet 109:149–153.

Fernandez BA, Roberts W, Chung B, Weksberg R, Meyn S, Szatmari P, Joseph-George AM, Mackay S, Whitten K, Noble B, Vardy C, Crosbie V, Luscombe S, Tucker E, Turner L, Marshall CR, Scherer SW. 2010. Phenotypic spectrum associated with de novo and inherited deletions and duplications at 16p11.2 in individuals ascertained for diagnosis of autism spectrum disorder. J Med Genet 47:195–203.

Finelli P, Natacci F, Bonati MT, Gottardi G, Engelen JJ, de Die-Smulders CE, Sala M, Giardino D, Larizza L. 2004. FISH characterisation of an identical (16)(p11.2p12.2) tandem duplication in two unrelated patients with autistic behaviour. J Med Genet 41:e90.

Girirajan S, Rosenfeld JA, Cooper GM, Antonacci F, Siswara P, Itsara A, Vives L, Walsh T, McCarthy SE, Baker C, Mefford HC, Kidd JM, Browning SR, Browning BL, Dickel DE, Levy DL, Ballif BC, Platky K, Farber DM, Gowans GC, Wetherbee JJ, Asamoah A, Weaver DD, Mark PR, Dickerson J, Garg BP, Ellingwood SA, Smith R, Banks VC, Smith W, McDonald MT, Hoo JJ, French BN, Hudson C, Johnson JP, Ozmore JR, Moeschler JB, Surti U, Escobar LF, El-Khechen D, Gorski JL, Kussmann J, Salbert B, Lacassie Y, Biser A, McDonald-McGinn DM, Zackai EH, Deardorff MA, Shaikh TH, Haan E, Friend KL, Fichera M, Romano C, Gécz J, DeLisi LE, Sebat J, King MC, Shaffer LG, Eichler EE. 2010. A recurrent 16p12.1 microdeletion supports a two-hit model for severe developmental delay. Nat Genet 42:203–209.

Hempel M, Rivera Brugués N, Wagenstaller J, Lederer G, Weitensteiner A, Seidel H, Meitinger T, Strom TM. 2009. Microdeletion syndrome 16p11.2-p12.2: Clinical and molecular characterization. Am J Med Genet A 149A:2106–2112.

Hernando C, Plaja A, Rigola MA, Pérez MM, Vendrell T, Egocue J, Fuster C. 2002. Comparative genomic hybridisation shows a partial de novo deletion 16p11.2 in a neonate with multiple congenital malformations. J Med Genet 39:e24.

Kumar RA, KaraMohamed S, Sudi J, Conrad DF, Brune C, Badner JA, Gilliam TC, Nowak NJ, Cook EH, Jr. Dobyns WB, Christian SL. 2008. Recurrent 16p11.2 microdeletions in autism. Hum Mol Genet 17:628–638.

Marshall CR, Noor A, Vincent JB, Lionel AC, Feuk L, Skaug J, Shago M, Moessner R, Pinto D, Ren Y, Thiruvahindrapduram B, Fiebig A, Schreiber S, Friedman J, Ketelaars CE, Vos YJ, Ficicioglu C, Kirkpatrick S, Nicolson R, Sloman L, Summers A, Gibbons CA, Teebi A, Chitayat D, Weksberg R, Thompson A, Vardy C, Crosbie V, Luscombe S, Baatjes R, Zwaigenbaum L, Roberts W, Fernandez B, Szatmari P, Scherer SW. 2008. Structural variation of chromosomes in autism spectrum disorder. Am J Hum Genet 82:477–488.

Tabet AC, Pilorge M, Delorme R, Amsellem F, Pinard JM, Leboyer M, Verloes A, Benzacken B, Betancur C. 2012. Autism multiplex family with 16p11.2p12.2 microduplication syndrome in monozygotic twins and distal 16p11.2 deletion in their brother. Eur J Hum Genet 20:540–546.

Weiss LA, Shen Y, Korn JM, Arking DE, Miller DT, Fossdal R, Saemundsen E, Stefansson H, Ferreira MA, Green T, Platt OS, Ruderfer DM, Walsh CA, Altshuler D, Chakravarti A, Tanzi RE, Stefansson K, Santangelo SL, Gusella JF, Sklar P, Wu BL, Daly MJ, Autism Consortium. 2008. Association between microdeletion and microduplication at 16p11.2 and autism. N Engl J Med 358:667–675.

nature COMMUNICATIONS

ARTICLE

Received 8 Oct 2013 | Accepted 30 Apr 2014 | Published 2 Jun 2014

DOI: 10.1038/ncomms5011

De novo SOX11 mutations cause Coffin–Siris syndrome

Yoshinori Tsurusaki[1,*], Eriko Koshimizu[1,*], Hirofumi Ohashi[2], Shubha Phadke[3], Ikuyo Kou[4], Masaaki Shiina[5], Toshifumi Suzuki[1,6], Nobuhiko Okamoto[7], Shintaro Imamura[8], Michiaki Yamashita[8], Satoshi Watanabe[9], Koh-ichiro Yoshiura[9], Hirofumi Kodera[1], Satoko Miyatake[1], Mitsuko Nakashima[1], Hirotomo Saitsu[1], Kazuhiro Ogata[5], Shiro Ikegawa[4], Noriko Miyake[1] & Naomichi Matsumoto[1]

Coffin–Siris syndrome (CSS) is a congenital disorder characterized by growth deficiency, intellectual disability, microcephaly, characteristic facial features and hypoplastic nails of the fifth fingers and/or toes. We previously identified mutations in five genes encoding subunits of the BAF complex, in 55% of CSS patients. Here we perform whole-exome sequencing in additional CSS patients, identifying *de novo SOX11* mutations in two patients with a mild CSS phenotype. *sox11a/b* knockdown in zebrafish causes brain abnormalities, potentially explaining the brain phenotype of CSS. SOX11 is the downstream transcriptional factor of the PAX6–BAF complex, highlighting the importance of the BAF complex and SOX11 transcriptional network in brain development.

[1] Department of Human Genetics, Yokohama City University Graduate School of Medicine, 3-9 Fukuura, Kanazawa-ku, Yokohama 236-0004, Japan. [2] Division of Medical Genetics, Saitama Children's Medical Center, 2100 Magome, Iwatsuki 339-8551, Japan. [3] Department of Medical Genetics, Sanjay Gandhi Postgraduate Institute of Medical Sciences, Raebareli Rd, Lucknow 226014, India. [4] Laboratory for Bone and Joint Diseases, Center for Integrative Medical Sciences, RIKEN, 4-6-1 Shirokanedai, Minato-ku, Tokyo 108-8639, Japan. [5] Department of Biochemistry, Yokohama City University Graduate School of Medicine, 3-9 Fukuura, Kanazawa-ku, Yokohama 236-0004, Japan. [6] Department of Obstetrics and Gynecology, Juntendo University, Hongo 3-1-3, Bunkyo-ku, Tokyo 113-8431, Japan. [7] Department of Medical Genetics, Osaka Medical Center and Research Institute for Maternal and Child Health, 840 Murodo-cho, Izumi 594-1101, Japan. [8] National Research Institute of Fisheries Science, 2-12-4 Fukuura, Kanazawa-ku, Yokohama 236-8648, Japan. [9] Department of Human Genetics, Nagasaki University Graduate School of Biomedical Sciences, 1-12-4 Sakamoto, Nagasaki 852-8523, Japan. * These authors contributed equally to this work. Correspondence and requests for materials should be addressed to N.M. (email: naomat@yokohama-cu.ac.jp).

Coffin–Siris syndrome (CSS; MIM#135900) is a congenital disorder characterized by growth deficiency, intellectual disability, microcephaly, characteristic facial features and hypoplastic nails of the fifth fingers and/or toes (Supplementary Fig. 1). Five subunit genes (*SMARCB1*, *SMARCA4*, *SMARCE1*, *ARID1A* and *ARID1B*) of the BAF complex (also known in yeast as the SWI/SNF complex[1]) are mutated in 55–70% of CSS patients[2–6]. Mutations in *SMARCA2*, another BAF complex gene, were reported in the Nicolaides–Baraitser syndrome, which is similar to, but distinct from CSS[7]. Furthermore, *de novo PHF6* mutations were found in two CSS patients[6], although no direct interaction has been reported between the BAF complex and PHF6, which interacts with the nucleosome remodelling and deacetylation complex[6]. As 30–45% of CSS patients were genetically undiagnosed in three large cohort studies[2–6], further genetic investigation is required to fully address the genetic picture of CSS.

Here we apply whole-exome sequencing (WES) to 92 CSS patients, and identify two *de novo SOX11* mutations in two unrelated patients. *sox11* knockdown experiments in zebrafish result in a smaller head and significant mortality, which were partially rescued by human wild-type *SOX11* messenger RNA (mRNA), but not by mutant mRNA.

Results

WES of CSS patients. We identified two *de novo SOX11* mutations in two unrelated patients, c.347A>G (p.Tyr116Cys) (in patient 1) and c.178T>C (p.Ser60Pro) (in patient 2) (deposited to LOVD, http://www.LOVD.nl/SOX11), among 92 CSS patients (including our previous cohorts[2,3]) analysed by trio-based WES. In the two patients, >10 reads covered 94–92% of coding sequences and only *SOX11* mutations remained as candidate variants in both of them based on the *de novo* model with scores of damaging or disease causing by SIFT, PolyPhen2 and Mutation Taster (Supplementary Table 1). The two heterozygous mutations localize to the high-mobility group (HMG) domain. Neither mutation was registered in the databases examined (1,000 Genomes, Exome Sequencing project (ESP) 6500, and in-house databases containing 575 control exomes) (Supplementary Table 1). We identified a further 22 *SOX11* variants within these three databases, but all of them reside outside the HMG domain and, based on prediction programs, are less likely to be pathogenic (Supplementary Table 1; Supplementary Fig. 2). The amino acids altered in SOX11 are evolutionarily conserved from zebrafish to human (Fig. 1). The mutations do not alter nuclear localization of SOX11 protein (Supplementary Fig. 3). *De novo* mutations were confirmed in the two families by Sanger sequencing along with biological parentage. No mutations in any of the other BAF complex genes, *PHF6*, or other potential candidate genes were found in the two families. Therefore, the two mutations identified are highly likely to be pathogenic. Moreover, *SOX11* was sequenced by WES ($n=23$) or Sanger method ($n=67$) in a further 90 CSS patients, with no mutations found. Fifty-four patients had a mutation in one of the five BAF complex subunit genes (58.7%) (*SMARCA4, SMARCB1, SMARCE1, ARID1A* and *ARID1B* mutations found in 9, 8, 1, 5 and 31 patients, respectively).

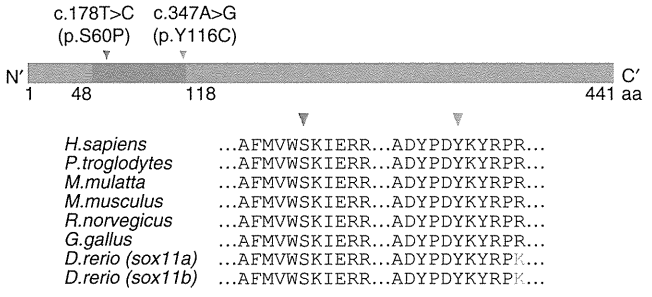

Figure 1 | *SOX11* mutations and functional characterization. *SOX11* mutations in CSS patients. Two missense mutations in the HMG domain (blue box) occur at evolutionarily conserved amino acids.

Clinical features of patients with *SOX11* mutations. The two patients showed dysmorphic facial features, microcephaly, growth deficiency, hypoplastic fifth toe nails and mild intellectual disability[8] (Supplementary Fig. 1; Supplementary Table 2). The observed clinical features in both patients are classified to a mild end of CSS as patient 1 spoke early for CSS and patient 2 has relatively high intelligence quotient. Although the two patients do not look similar in facial appearance (patient 1 has midface hypoplasia, while patient 2 does not; in addition there is an ethnic difference, as patients were either Japanese or Indian), they do share features in common, namely, hypertrichosis, arched eyebrows, low-set ears, auricular back-rotationand full cheeks (Supplementary Fig. 1).

Patient 1 (Japanese) was born at 38 weeks of gestation following an uneventful pregnancy. Her birth weight was 2,340 *g* (−1.9 s.d.), length 45 cm (−2.2 s.d.) and occipitofrontal circumference (OFC) 30.5 cm (−1.8 s.d.). She was hypotonic, had feeding difficulties (especially during the neonatal period) and delayed development. She was able to support her head at 5 months of age, sit at 11 months and walk independently at 1 year 11 months. She started to speak meaningful words at 1 year 7 months. At 3 years, her developmental quotient was estimated using the Kyoto scale of psychological development to be 57. Abdominal echography showed her left kidney was slightly small in size. She has distinctive facial features characterized by midface hypoplasia, short palpebral fissures, hypertelorism, upturned palpebral fissures, long eyelashes, a low nasal root, shortened nose with upturned nostrils, short philtrum, open mouth, full lips and low-set ears. Hypoplastic distal phalanges with nail hypoplasia (especially of the fifth digits) were also noted. Additional findings included hypertrichosis and long eyelashes with abundant hair on the scalp. At 4 years 8 months, she was short with a height of 92.1 cm (−2.9 s.d.) and evaluated for possible growth hormone deficiency with stimulation tests, which showed normal results. At 10 years, she measured 119 cm (−2.8 s.d.), weighed 20.1 kg (−1.8 s.d.) and had an OFC of 47.3 cm (−3.3 s.d.). She attends a special education class for poor performance, but can walk to school by herself (takes approximately half an hour) and is able to communicate verbally, to some extent, with her classmates. Clinical features are summarized in Supplementary Table 2.

Patient 2 (Indian) is a 16-year-old female, and was referred to the genetics outpatient department for evaluation of short stature. She was born at term following a normal pregnancy, but with low birth weight (1.75 kg, −4s.d.). Developmental milestones were attained normally, but her parents always felt that she lagged behind other children. She was a slow learner with poor scholastic performance and an intelligence quotient of 70–80. She attended a normal class, but struggled to pass class examinations every year. She has a proportionately short stature but not a coarse face. Her chin was small and supraorbital ridges hypoplastic with no ptosis. Her nose was long and alae nasi hypoplastic with overhanging columella. Her hair was thick and rough with some thinning on her scalp. She had increased hair on her back. Her fourth and fifth toes were short and all her finger nails were hypoplastic with thin and tapered fingers. Her fourth and fifth toes on both feet, and also the third toe on her right foot, were

markedly hypoplastic. Clinodactyly was noted on the third, fourth and fifth toes on her right foot, and the third and fourth toes on her left foot. A skeletal survey did not show any radiographic bone abnormalities. Her bone age was 13–14 years and follicle-stimulating hormone was 1.57 $IU l^{-1}$ (normal range: <5 $IU l^{-1}$). Ultrasonographic examination at 16 years (before menarche), showed a hypoplastic uterus and malrotation of both kidneys. No secondary sexual characteristics were recognized until she had menarche at 17 years. Now at age of 17 years, she is still short with a height of 141 cm (-5 s.d.), weigh 31.3 kg (-3 s.d.) and OFC 50.5 cm (-4.5 s.d.). Clinical features are summarized in Supplementary Table 2.

Structural effects of SOX11 mutations. To determine the impact of the disease-causing mutations on human SOX11 structure and function, we mapped the mutation positions onto the crystal structure of mouse Sox4[9], that is analogous to human SOX11, and calculated free energy changes on the mutations using FoldX software[10,11]. The mutations lie in the highly conserved HMG domain, responsible for sequence-specific DNA binding (Fig. 2a)[9]. Ser60 is located in a helix of the HMG domain (Fig. 2a), therefore the S60P mutation may affect overall folding of the HMG domain and impair DNA binding of SOX11. FoldX calculations supported this prediction and the free energy change on the mutation was high enough to destabilize protein folding (>10 kcal mol^{-1}) (Fig. 2b)[12]. Conversely, Tyr116 forms a hydrophobic core with the side chains of DNA-recognition loops (Fig. 2a). The Y116C mutation has low free energy change (<1 kcal mol^{-1}) (Fig. 2b), and is unlikely to significantly affect folding of the HMG domain, but instead may alter conformation of the DNA-recognition loop, which is important for DNA binding.

***SOX11* mutations affect downstream transcription.** Both mutations are located within the HMG domain, which is required for *SOX11* transcriptional regulation of *GDF5* (ref. 13). Luciferase assays using the *GDF5* promoter in HeLa and ATDC5 cells, showed both mutant proteins had decreased transcriptional activities compared with wild type (WT) (Fig. 3).

SOX11 expression. *SOX11* transcription levels were examined using multiple human complementary DNA (cDNA) panels. *SOX11* was exclusively expressed in brain (foetus and adult) and heart (adult) tissues, supporting a role for *SOX11* mutations in the brain features of CSS observed in the two patients (Supplementary Fig. 4; Supplementary Table 2).

In mice, targeted *Sox11* disruption with a β-galactosidase marker gene results in 23% birth weight reduction and lethality after the first postnatal week in homozygotes, due to hypoplastic lungs and ventricular septation defects. In addition, skeletal malformations (including phalanges) and abdominal defects are observed[14]. Physical and functional abnormalities in heterozygotes have not been described. However, in heterozygous mice, β-galactosidase expression revealed early ubiquitous expression throughout the embryo with upregulation in the central nervous system (CNS) and limb buds[14].

***sox11* knockdown experiments in zebrafish.** We further investigated *sox11* function in zebrafish. The zebrafish genome contains two orthologs of human *SOX11*, *sox11a* and *sox11b*, which are expressed in all cells until gastrulation and later become restricted to the developing CNS[15,16]. We knocked down zebrafish *sox11a* and *sox11b* (both single-exon genes) using translation-blocking morpholino oligonucleotides (MOs) (*sox11a*-MO, *sox11b*-MO and *sox11a/b*-MO), as previously described[17] (Supplementary Fig. 5a). Off-target effects of morpholino injections were excluded by repeated experiments, co-injecting with *tp53* MO or injecting into $tp53^{zdf1/zdf1}$ mutant fish[18,19]. *sox11a*- and *sox11b*-MO knockdown caused similar phenotypes, including smaller heads and body curvature (Supplementary Fig. 5b). Low-dose *sox11a*- (1.6 ng), *sox11b*- (1.6 ng) and *sox11a/b*- (1.6 ng) MO-injected embryos resulted in

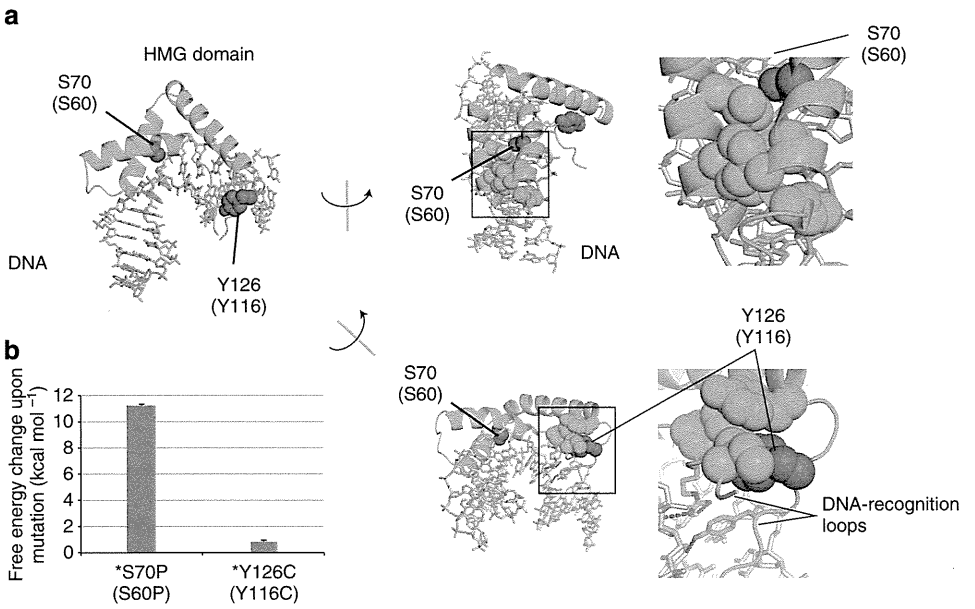

Figure 2 | Structural effects of SOX11 mutations. (**a**) Crystal structure of the mouse Sox4 HMG domain bound to DNA. Helices and loops are shown as green ribbons and threads, respectively. DNA is shown as grey sticks. Amino-acid residues at mutation sites are shown coloured red in the space-filling model. In the middle and right images, some of the amino-acid residues involved in the hydrophobic core surrounding mutation points are shown coloured green in the space-filling model. Amino-acid numbering is indicated for mouse Sox4 with that for human SOX11 in parentheses. Hydrogen bonds are shown as black dotted lines. Molecular structures were drawn using PyMOL (http://www.pymol.org). (**b**) Free energy changes on the indicated mutations calculated by FoldX software.

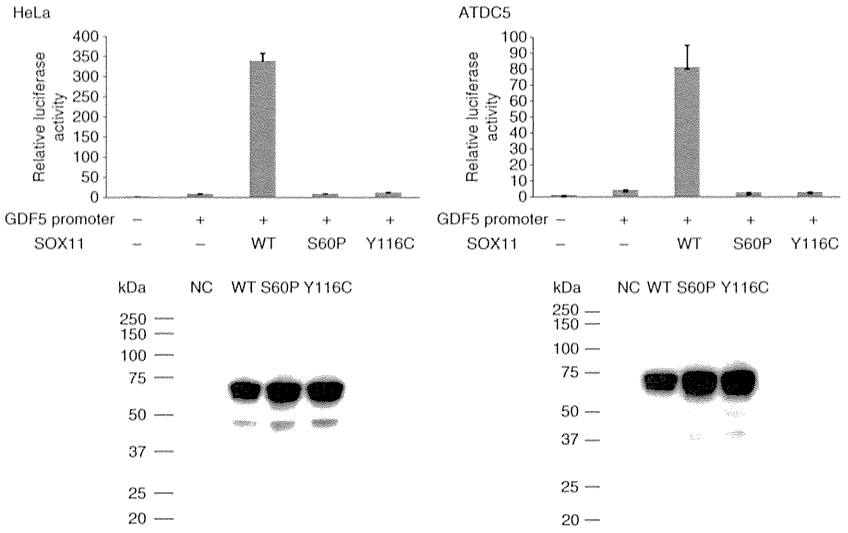

Figure 3 | *SOX11* mutations affecting *GDF5* promoter activity. Luciferase reporter assays measured transcriptional activity of the *GDF5* promoter (−448/+319) (UCSC genome browser hg19: chr20: 34025709-34026457) in HeLa (left) and ATDC5 (right) cells. HeLa or ATDC5 cells were co-transfected with WT or mutant (S60P and Y116C) SOX11 expression vector and reporter constructs containing either GDF5 promoter or empty vector (pGL3-basic). Relative luciferase activities compared with empty vector are presented as mean ± s.d. for two independent experiments, with each experiment performed in triplicate (upper). Immunoblot analysis of transfected HeLa and ATDC5 cell extracts showing wild-type (WT) or mutant (S60P and Y116C) SOX11 proteins (lower). Compared with WT, both SOX11 mutants reduced *GDF5* transcriptional activities in HeLa and ATDC5 cells.

significant mortality (*sox11a*-MO, ~49.3%; *sox11b*-MO, ~19.3%; *sox11a/b*-MO, ~53.0%), compared with control-MO embryos (~7.3%) (Fig. 4a). Co-injection of WT human *SOX11* mRNA (h*SOX11*-WT mRNA) with *sox11a/b*-MO improved morphant survival at 48 h post fertilization (hpf) (25.5% lethality versus 49.3% lethality with *sox11a/b*-MO alone) ($P<0.01$) (Fig. 4a; Supplementary Fig. 5c). The affected phenotype of *sox11a/b* double morphants was partially rescued by h*SOX11*-WT mRNA overexpression (4.5% normal for *sox11a/b*-MO alone versus 36.5% for co-injection with h*SOX11*-WT mRNA and *sox11a/b*-MO, $P<0.01$) (Fig. 4a). In contrast, co-injection of either mutant h*SOX11* mRNA (h*SOX11*-S60P and -Y116C mRNA) with *sox11a/b*-MO showed no significant rescue effects on lethal and affected phenotypes (Fig. 4a). There were significantly more normal phenotypes following h*SOX11*-WT mRNA and *sox11a/b*-MO co-injection, than with h*SOX11*-mutant mRNA co-injections ($P<0.05$). Head sizes in randomly selected embryos ($n\geq10$) of *sox11a* and *sox11a/b* morphants at 48 hpf were significantly decreased ($P<0.05$ in both), but not significantly changed in *sox11b* morphant. Overexpression of h*SOX11*-WT mRNA restores *sox11a/b* double-morphant head size (in randomly selected embryos, $n\geq10$), suggesting specific *sox11* suppression by morpholino injection (Fig. 4b). Although the head size of h*SOX11*-mutant mRNA and *sox11a/b*-MO-injected embryos was slightly decreased, no significant difference was recognized between overexpression of h*SOX11*-WT or h*SOX11*-mutant mRNA and *sox11a/b*-MO co-injection (Fig. 4b).Staining with acridine orange and terminal deoxynucleotidyl TdT-mediated dUTP nick end labelling (TUNEL), found significant apoptotic increases exclusively in microcephalic embryos (Fig. 4c; Supplementary Fig. 6). Brain cell death was prevented by co-injection with h*SOX11*-WT mRNA, but not by mutant h*SOX11* mRNAs (Fig. 4c). We also used HuC/D (a marker for early postmitotic and mature neurons) and acetylated tubulin (an axonal marker) immunostaining at 48 hpf to analyse neuronal cells in more detail (Supplementary Fig. 7). Decreased HuC/D-positive neurons, especially in the telencephalon and diencephalon, were observed in *sox11* morphants (Supplementary Fig. 7a). The phenotype in *sox11a/b*-MO-injected embryos was efficiently rescued by h*SOX11*-WT mRNA (Supplementary Fig. 7a). Reduction of HuC/D-positive neurons was unaltered by mutant h*SOX11* mRNA overexpression and *sox11a/b*-MO injection (Supplementary Fig. 7a). Anti-acetylated tubulin staining also showed severely reduced axonal numbers in the forebrain, midbrain and hindbrain of *sox11* morphants, compared with control-MO-injected embryos (Supplementary Fig. 7b). *sox11a/b* morphants showed phenotypic rescue when co-injected with h*SOX11*-WT mRNA, compared with mutant h*SOX11* mRNAs (Supplementary Fig. 7b).

Discussion

We have identified *SOX11* mutations in CSS. This is the first report of human mutations in *SOXC* (*SOX4*, *SOX11* and *SOX12*)[20]. *SOX11*/*sox11* is required for neurogenesis, and loss of function in early embryos is sufficient to impair normal CNS development. Haploinsufficiency of other *SOX* genes (*SOX2*, *SOX9* and *SOX10*) is known to cause human diseases[21–23]. It is interesting that mutations of *SOX11* and other BAF subunit genes are mutually exclusive in CSS.

Sox11 was recently shown to form a transcriptional cross-regulatory network downstream of the Pax6–BAF complex. The network drives neurogenesis and converts postnatal glia into neurons[24]. Brg1 (Smarca4) binds to the *Sox11* promoter, and interaction with Pax6 is sufficient to induce Sox11 expression in neurosphere-derived cells in a Brg1-dependent manner[24]. Therefore, the Pax6–BAF complex activates a cross-regulatory transcriptional network, maintaining high expression of genes involved in neuronal differentiation and execution of cell lineage decisions[24]. *SOX11* mutations appear to be a rare cause of CSS as only 2 out of 92 patients (2.2%) showed *SOX11* abnormality and to be limited to the mild end of CSS phenotype. Abnormality of the upstream BAF complex tends to show a more severe phenotype compared with that of a downstream *SOX11* mutation, which may indicate rather specific effects of *SOX11* mutations on the CSS phenotype.